

SEPTIEME COLLOQUE SUR LE TRAITEMENT DU SIGNAL ET SES APPLICATIONS

NICE du 28 MAI au 2 JUIN 1979

Calculation and measurements of holograms and numerical reconstruction of images in the microwave region

F. Arndt, P. Ballerscheff, K.-H. Schierenbeck

Department of microwaves, University of Bremen, Kufsteiner Strasse,
D-2800 Bremen 33, W-Germany.

RESUME

Dans cet exposé la distribution des hologrammes et la reconstruction des images des objets quelconques est analysée numériquement et expérimentalement. La qualité de la reconstruction numérique des images est évidemment perfectionnée par une propre expansion des hologrammes et par la considération du théorème d'analyse discrète. La calculation des hologrammes est éprouvée par des mesurages pour quelques exemples. La propre reconstruction des images des objets d'une forme compliquée et qui sont posés en distances différents indique qu'une identification claire des objets est possible.

SUMMARY

The paper investigates numerically and experimentally the distribution of holograms in the microwave region for arbitrary objects and the numerical reconstruction of images. By suitable expansion of the hologram and by consideration of the sampling theorem a clear improvement in the quality of the numerical reconstruction of images is obtained. Some examples of the numerically simulated holograms were proved by measurements. The suitable imaging reconstruction of objects with a complicated contour and which are arranged at different distances show that clear identification of the objects is possible.



Calculation and measurement of holograms and numerical reconstruction of images in the microwave region

1. Introduction

In microwave holography the known principles of optics are applied to the microwave region with the objective of endeavouring to identify radar targets with regard to their geometrical shape [1]-[7]. The papers [1]-[7] can be separated into two groups. The first is called "multifrequency quasi-holography" [1]-[3] where cylindrical objects in the vicinity of the radar antenna are analyzed with the aid of a phase spectrum. The following paper is a contribution to the improvement of the holography techniques of the second group [4]-[7] where the diffraction theory of a plane object is used. As in optics the information is stored as a hologram. The restriction of near objects is unnecessary.

In this paper it is shown firstly that a computer simulation of holograms for arbitrary (Fig. 1) objects is possible using the Fresnel-Kirchhoff's diffraction integral. For three dimensional objects it is convenient to subdivide the z-dimension into suitable parts so that the plane diffraction theory can be used approximately. The advantage of this numerical simulation is that the necessary expansion of the hologram and the sampling theory for spatial spectra can be systematically studied in order to improve the accuracy of the imaging method. By numerical reconstruction it can be shown that a clear improvement of the imaging quality is obtained. Experimental results show that reliable identification of the object is possible.

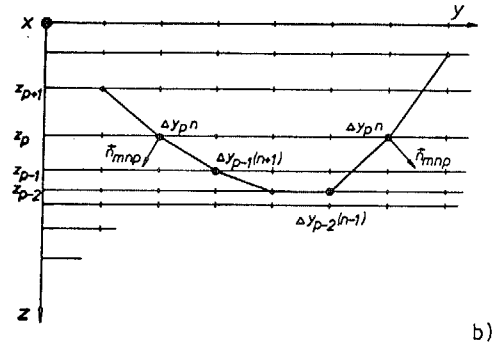


Fig. 1

Object and hologram plane

2. Diffraction theory

The Fresnel-Kirchhoff's diffraction integral [8] for the arbitrary case where the diffraction interface (or the diffracting hole, respectively, using Babinet's principle) is not plane can be written in the form:

$$\underline{U}(x_0, y_0) = j \frac{1}{2\lambda} \iint_B \frac{e^{-jkr}}{r} \cdot \frac{e^{-jks}}{s} \cdot \underline{B}(x, y) \cdot [\cos\{\vec{n}, \vec{r}\} - \cos\{\vec{n}, \vec{s}\}] dx dy \quad (1)$$

where

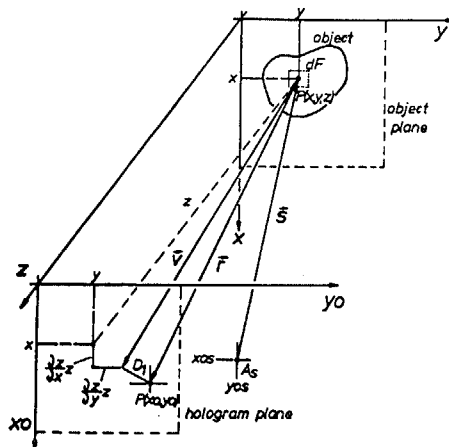
$\underline{U}(x_0, y_0) \sim E_y(x_0, y_0)$ = complex amplitude factor of the diffracted wave at the point P(x₀, y₀) in the hologram plane, (Fig.1),

\vec{n} = direction of the area dF,

λ = wave-length,

$k = 2\pi/\lambda$,

$\underline{B}(x, y)$ = complex field distribution of the diffracting interface,



a)

$$r = \sqrt{(x_0 - x)^2 + (y_0 - y)^2 + z^2}$$

$$s = \sqrt{(x_{0s} - x)^2 + (y_{0s} - y)^2 + z^2}$$

with the restrictions that the diffracted field is assumed to be not too far away from the z-axis, that the angles $\{\vec{z}, \vec{r}\}$, $\{\vec{z}, \vec{s}\}$ are small, and that the dimensions of the diffracting objects as well as r and s are large with regard to the wavelength λ .

Calculation and measurement of holograms and numerical reconstruction of images in the microwave region

To determine the cosine terms in Equation (1) we define a vector $\vec{v} = \vec{n} \cdot v$ with

$$v = [1 + (\frac{\partial z}{\partial x})^2 + (\frac{\partial z}{\partial y})^2] \cdot z \quad (2)$$

and use the cosine theorem

$$\cos\{\vec{n}, \vec{r}\} = \cos\{\vec{v}, \vec{r}\} = \frac{r^2 + v^2 - D_1^2}{2rv}$$

$$\cos\{\vec{n}, \vec{s}\} = \cos\{\vec{v}, \vec{s}\} = -\frac{s^2 + v^2 - D_2^2}{2rv}$$

with

$$D_1^2 = (x_o - x - \frac{\partial z}{\partial x} z)^2 + (y_o - y - \frac{\partial z}{\partial y} z)^2$$

$$D_2^2 = (x_{os} - x - \frac{\partial z}{\partial x} z)^2 + (y_{os} - y - \frac{\partial z}{\partial y} z)^2$$

3. Discrete representation of the diffraction integral

The z-dimension of the object (Fig. 1) is subdivided into P planes with the dimensions $\Delta x_p \cdot M$ and $\Delta y_p \cdot N$ (Fig. 1b). P is chosen to be 9. z_p is the distance to the hologram plane. Equation (2) is then given in its discrete form:

$$\underline{U}_{il} = j \frac{1}{2\lambda} \sum_{p=1}^P \Delta x_p \Delta y_p \sum_{m=0}^{M-1} \sum_{n=0}^{N-1} O_{mnp} \cdot C_s \cdot \frac{e^{-jk s_{mnp}}}{s_{mnp}} \cdot \frac{e^{-jk r_{mnilp}}}{r_{mnilp}} \cdot [\cos\{\vec{v}_{mnp}, \vec{r}_{mnilp}\} - \cos\{\vec{v}_{mnp}, \vec{s}_{mnp}\}] \quad (3)$$

where

O_{mnp} = object function of the reflecting object (e.g. for a rectangular plate $O_{mnp} = 1$).

$$s_{mnp} = [(x_{os} - \Delta x_p m)^2 + (y_{os} - \Delta y_p n)^2 + z_p^2]^{1/2}$$

$$r_{mnilp} = [(\Delta x_{oi} - \Delta x_p m)^2 + (\Delta y_{oi} - \Delta y_p n)^2 + z_p^2]^{1/2}$$

C_s = constant of the radiating set (it can be for instance chosen to be 1m since only relative results are of interest).

The cosine terms in Equation (3) can be expressed similar as in Equation (2) where $\frac{\partial z}{\partial x}$ and $\frac{\partial z}{\partial y}$ are replaced by the differences

$$\frac{\partial z}{\partial x} \approx \frac{z_p - z_{p-k}}{\Delta x_p m - \Delta x_{p-k}(m \pm 1)} ; \quad \frac{\partial z}{\partial y} \approx \frac{z_p - z_{p-k}}{\Delta y_p n - \Delta y_{p-k}(n \pm 1)}$$

We define

$$\nu = \frac{x_o}{\lambda z} \quad \mu = \frac{y_o}{\lambda z} \quad (4)$$

(x_o, y_o o.f. Fig. 1).

The sampling theorem for the sample point distance $\Delta x, \Delta y$ in the object plane and the sample point distance $\Delta x_o, \Delta y_o$ in the hologram plane leads to

$$\begin{aligned} \Delta x &\leq \frac{1}{\Delta \nu I} = \frac{\lambda z}{I} \cdot \frac{1}{\Delta x_o} \\ \Delta y &\leq \frac{1}{\Delta \mu L} = \frac{\lambda z}{L} \cdot \frac{1}{\Delta y_o} \\ \Delta \nu &\leq \frac{1}{\Delta x \cdot M} ; \quad \Delta \mu \leq \frac{1}{\Delta y \cdot N} \end{aligned} \quad (5)$$

where I, L is the number of the samples points in the hologram plane and M, N is the number of the sample points in the object plane.

For rectangular objects the dimensions of the hologram should be

$$x_{oI} \geq \frac{2 \cdot \eta \cdot \lambda \cdot z}{x_{obj}} ; \quad y_{oL} \geq \frac{2 \cdot \eta \cdot \lambda \cdot z}{y_{obj}}$$



Calculation and measurement of holograms and numerical reconstruction of images in the microwave region

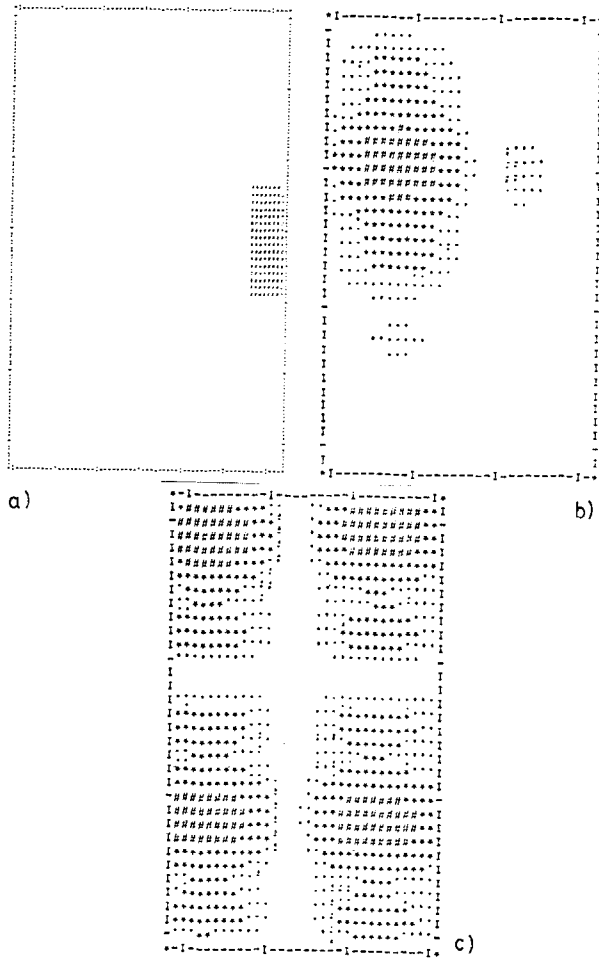
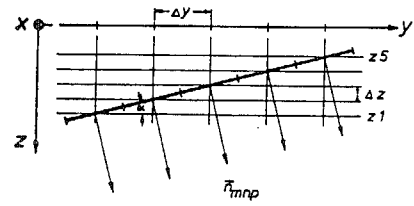
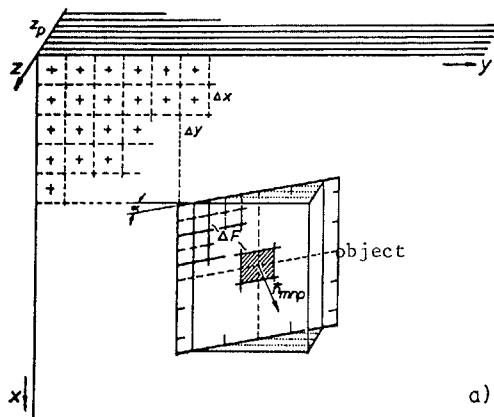


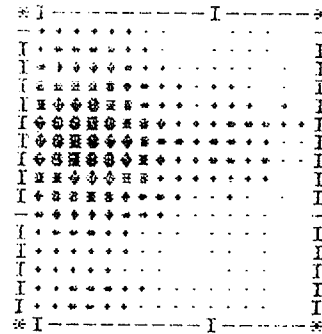
Fig. 2

Hologram simulation of a plane object

Fig. 2b shows the numerically simulated amplitude hologram according to Equation (3) of a plane rectangular object (c.f. Fig. 2a) if the sampling theorem (5) is held. If the sampling theorem is not held the hologram is distorted (Fig. 2c). For a rectangular object inclined in the z direction with an angle α (Figs. 3a, 3b) the amplitude hologram is given in Fig. 3c.



b)



c)

Fig. 3

Hologram simulation of an inclined object

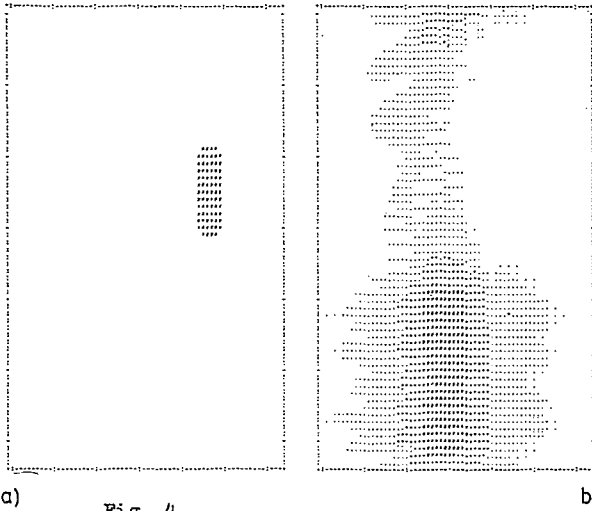
4. Reconstruction of images

For the numerical reconstruction it has been found to be adequate to use the Fresnel-transformation [4]

$$\begin{aligned}
 B_{mn} = & -j \frac{\Delta x_0 \Delta y_0}{\lambda z} \exp(jkz) \cdot \\
 & \cdot \exp\left\{j\pi\lambda z \left[\left(\frac{m}{\Delta x_0 M}\right)^2 + \left(\frac{n}{\Delta y_0 N}\right)^2\right]\right\} \\
 & \cdot \sum_{i=0}^{I-1} \sum_{l=0}^{L-1} \underbrace{U_{il} \exp\left\{j\frac{\pi}{\lambda z} [(\Delta x_0 i)^2 + (\Delta y_0 l)^2]\right\}}_{G_{il}} \\
 & \cdot \exp\left[-j2\pi\left(\frac{i m}{M} + \frac{l n}{N}\right)\right] .
 \end{aligned} \tag{6}$$

Equation (6) is a two dimensional discrete Fourier-transform of the function G_{il} . If I and L are powers of the base 2 the fast Fourier-transform can be used.

Calculation and measurement of holograms and numerical reconstruction of images in the microwave region



a) Fig. 4
Numerical reconstruction of images

As an example Fig. 4a shows the reconstruction of the hologram of Fig. 2b for the plane rectangular object. In Fig. 4b the sampling theorem for the hologram plane is not satisfied and we see that the object cannot be identified.

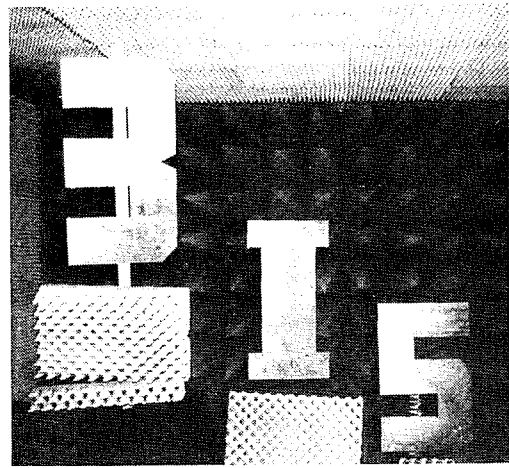
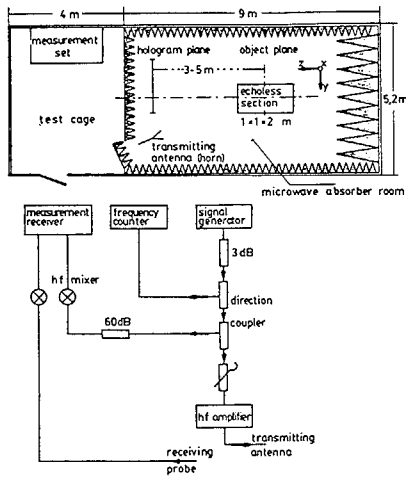
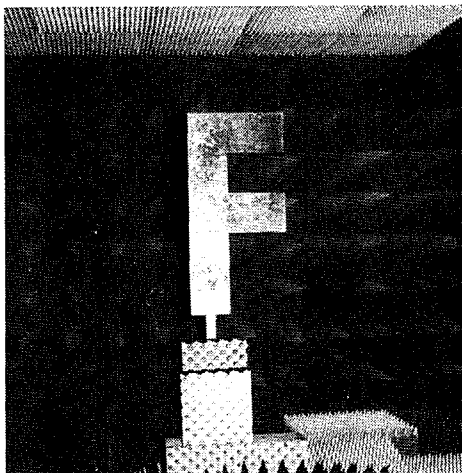


Fig. 5
Measuring arrangement and objects

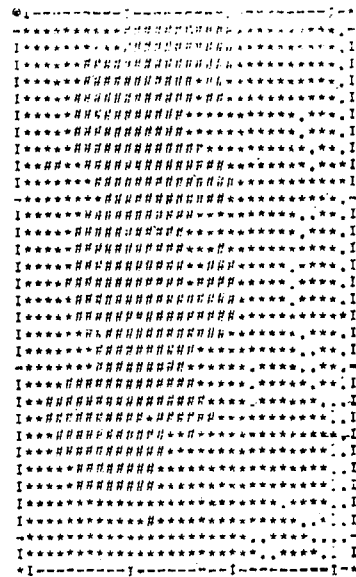
To prove the numerical simulation of the hologram and to demonstrate the possibility of identifying objects by suitable numerical reconstruction techniques the measuring arrangement of Fig. 5a was employed. The first example is a plane object with the contour "F" (Fig. 5b). The simulated hologram is given in Fig. 6a. There is practically no difference in the measured hologram (Fig. 6b). The reconstruction of the image stored in the measured hologram is shown in Fig. 6c.



a)



b)



6a)



Calculation and measurement of holograms and numerical reconstruction of images in the microwave region

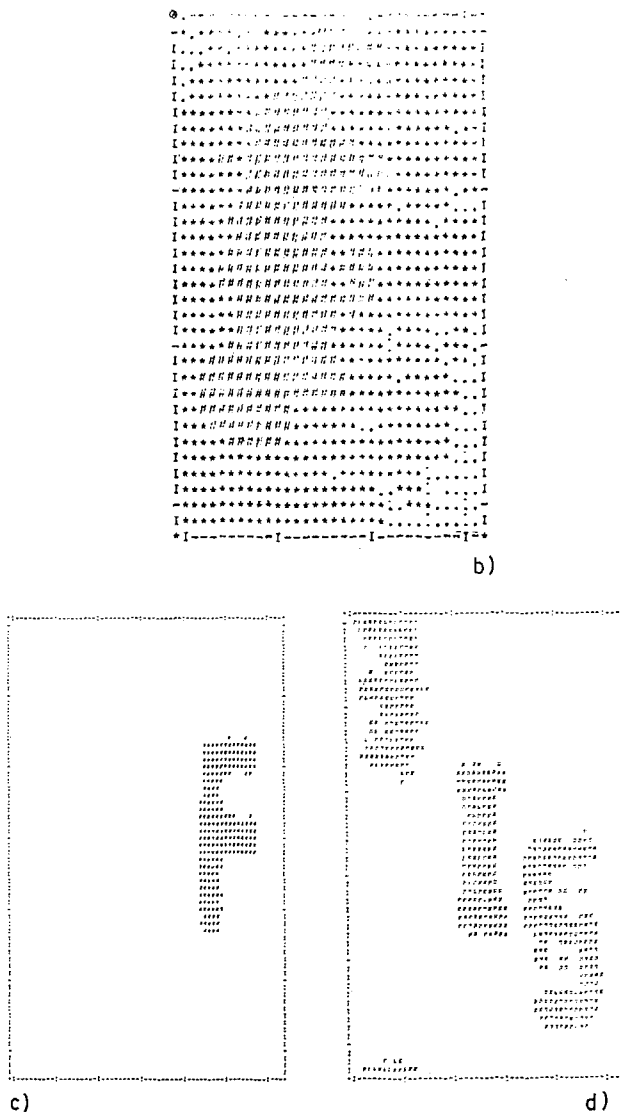


Fig. 6

Simulated and measured hologram of the object "F", reconstruction of the images

As a second example three objects were chosen with the contours "3 1 5" which were set up at different distances (Fig. 5c). Fig. 6d shows the numerical reconstruction of the image stored in the measured hologram. The quality of the reconstructed image permits the clear identification of the three objects.

References

- [1] Karg, R. und Ermert, H., Ein multi-frequentes, quasi-holographisches Abbildungssystem im Mikrowellenbereich. Nachrichtentech. Z. 27[1974], 369-372.
- [2] Karg, R., Multifrequent microwave holography at close range. Conf.Proc., 5th European Microwave Conf., Hamburg 1975, S. 208-212.
- [3] Karg, R., Multifrequency microwave holography. AEU 31 [1977], 150-156.
- [4] Aoki, Y., Optical and numerical reconstructions of images from sound-wave holograms. Transact. IEEE AU-18 [1970], 258-267.
- [5] Aoki, Y. and Boivin, A., Computer reconstruction of images from a microwave hologram. Proc. IEEE 58 [1970], 821-822.
- [6] Magura, K., Probleme bei der holographischen Abbildung im Mikrowellenbereich. Dissertation, Technische Hochschule Aachen, 1974.
- [7] Arndt, F., Ballerscheff, P., Schierenbeck, K.-H. and Ussat, H., Hologrammsimulation und Bildrekonstruktion bei der Mikrowellenholographie. AEU 32 [1978], 114-122.
- [8] Silver, S., Microwave antenna theory and design. McGraw-Hill Book Co., New York 1949.